International Journal of Multimedia and Ubiquitous Engineering
Vol. 10, No. 2 (2015), pp. 351-360
http://dx.doi.org/10.14257/ijmue.2015.10.2.32

Hyperspectral Image Compression and Reconstruction Based on Compressed Sensing

Xu Cheng[1], Huang Daqing[2] and Han Wei[3]

[1,3]*College of Electronic Information Engineering, Nanjing University of Aeronautics and Astronautics, Nanjing, China*
[2]*Research Institute of UAV, Nanjing University of Aeronautics and Astronautics, Nanjing, China*
[1]*stonejack2014@gmail.com*, [2]*nuaauav@126.com*, [3]*10238176@qq.com*

Abstract

According to the characteristics of hyperspectral images, a novel compression and reconstruction algorithm for hyperspectal images based on compressed sensing is proposed. The random measurements of each image and the linear prediction coefficients are made at the encoder, and then transmitted sequentially to the decoder. At the decoder, in terms of apparent correlations between the adjacent spectral bands, a de-correlation algorithm based on block linear prediction model is used in reconstruction process. The inter-band redundancies are removed from the measurements of current image, thus the de-correlation image data is sparser, which can be reconstructed easily. Experimental results show that the proposed algorithm achieves improved reconstruction performance and efficiently reduces the cost of computation at the encoder, which is more suitable for hardware implementation.

Keywords: *hyperspectral image, compressed sensing, inter-band prediction, image reconstruction*

1. Introduction

Hyperspectral imaging combines standard digital imaging with common spectroscopic methods, such as near-IR, visible and fluorescence imaging, to provide increased sensitivity and discrimination capabilities over traditional imaging and detection methods [1]. Hyperspectral sensors collect information as a set of images; each image represents a range of the electromagnetic spectrum and is also known as a spectral band. These images are then combined and form a three-dimensional hyperspectral data cube for processing and analysis. With the development of spectral imaging technology, spectral resolution and spatial resolution of the imaging spectrometer are continuously rising, and hyperspectral imaging is applied more widely in the field of aerospace. However, a significant problem is followed, namely, the amount of hyperspectral images increases dramatically. For example, each instance of the hyperspectral images acquired by the NASA's Airborne Visible InfraRed Imaging Spectrometer (AVIRIS) contains more than 140 MBytes of data. Such enormous amount of information brings serious challenges, particularly, to the embedded systems, such as spacecrafts, where the power consumption, memory storage, computational complexity and bandwidth are posing tight constraints on system implementation. Therefore, effective hyperspectral image compression technology is an urgent need to resolve this problem.

ISSN: 1975-0080 IJMUE

In this regard, many compression methods have been developed over the last twenty years to reduce the size of hyperspectral image, prior to storage or transmission. Among all those works, the fact needs to be focused that despite the huge size of hyperspectral image, there are massive correlations both spatially and spectrally. Thus exploiting them properly enables one to design efficient compression algorithms. Rao A K proposes an approach based on bidirectional inter-band prediction to remove spectral redundancies [2]. In addition, an adaptive 3-D wavelet transform coding is applied to compress hyperspectral images [3-4], which is more efficient than SPIHT (Set Partitioning in Hierarchical Trees) algorithm. However, these approaches have a common disadvantage that they lead to large memory consumption, computation complexity and it is difficult to achieve real-time image compression and transmission, and thus these approaches are not very suitable for hyperspectral image compression in the field of aerospace.

In recent years, compressed sensing (CS) has received much attention in the signal-processing field. The CS framework was introduced by Candes, *et al.,* in [5] and Donoho in [6]. CS theory enables sparse or compressible signals to be captured and stored at a rate much lower than the Nyquist rate. As long as the measurements satisfy certain conditions (such as incoherence, RIP), the recovery of the original signal from its randomized projections can be made possible by means of an optimization process. The CS theory can be applied to the field of image compression and reconstruction as well, because an image is sparse in some basis, especially the hyperspectral image, which often has smooth texture changes. The image can be reconstructed with high quality via simple random sampling at the encoder and ℓ_1-norm optimization at the decoder. CS has the characteristics of coding easily, decoding complicatedly, and it can reconstruct the image either exactly or with provably small probability of error. Recently, a few of novel approaches have been proposed based on the compressed sensing idea in order to reconstruct image by very small number of measurements. The authors of [7] apply iteratively reweighted algorithms for computing local minima of the non-convex problem. A particular regularization strategy is adopted to greatly improve the ability of a reweighted least-squares algorithm to recover images. In [8], the reconstruction approach is based on a convex minimization which penalizes both the nuclear norm and the $\ell_{2,1}$ mixed-norm of the data matrix. Thus, the solution tends to have a simultaneous low-rank and joint-sparse structure. Other approaches [9-11] have been developed in order to take advantage of both spectral and spatial correlations of hyperspectral image simultaneously.

In this paper, a novel hyperspectral image compression and reconstruction approach is proposed based on CS and the hyperspectral image spectral characteristics. Within this framework, an inter-band prediction model is built to reduce the correlation among adjacent hyperspectral images, which can effectively improve the image reconstruction quality. This method has slight coding complexity and can be easily implemented in embedded hardware, providing the possibility for the real-time coding and transmission for hyperspectral image sequences. This paper is organized as follows. Section II gives an overview on the proposed scheme firstly, and then introduces the basic compressed sensing theory, compressed sensing implement for hyperspectral image compression and reconstruction, block linear prediction model in detail. Numerical simulation results are given Section III. Section IV concludes the work.

2. Proposed Scheme

The characteristics of hyperspectral image are different from the general image. Hyperspectral images are obtained from the same place at different bands simultaneously, which result in high correlation between bands. The compression algorithm for general image cannot take full advantage of this characteristic of hyperspectral image, so the compression efficiency is rather low. In this case, a compressive sensing framework is designed for hyperspectral image compression and reconstruction based on inter-band prediction model, which can reduce the correlation among adjacent hyperspectral images. The overall block diagram is shown in Figure 1.

At the encoder, the current frame is observation projected and the linear prediction coefficients are calculated according to current frame and reference frame, where the reference frame is the previous frame image of the current frame. Furthermore, the prediction coefficients as auxiliary information are transmitted to the decoder. At the decoder, the predicted frame is obtained from the previous reconstructed frame with inter-band prediction model. Then the predicted frame is observation projected. The residual measurement vector is equal to the current frame measurement vector minus the predicted frame measurement vector. After reconstructing the residual image using GPSR (Gradient Projection for Sparse Reconstruction) algorithm [12], the current frame can be recovered combined with the predicted frame. Finally, the recovered image is stored in the frame memory, preparing for the next frame image reconstruction.

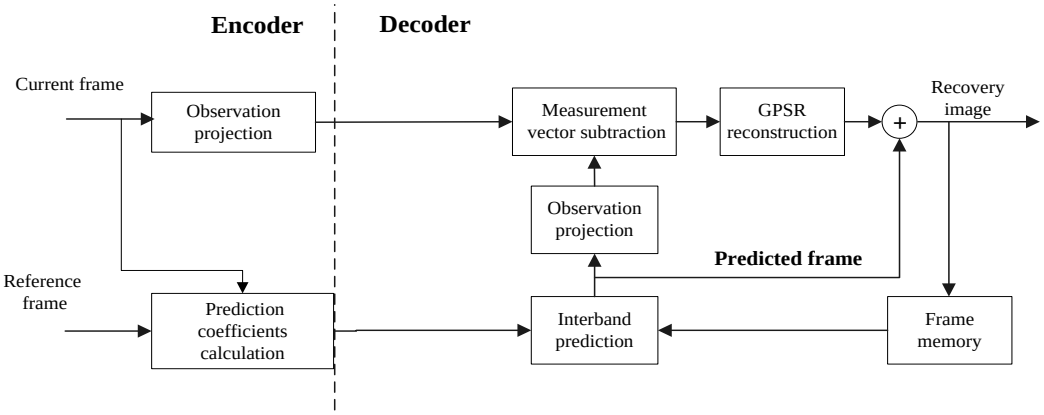

Figure 1. Scheme Structure

2.1. CS Basic Principles

To be able to outline the basic principles of CS, we first introduce some necessary definitions and notation. Signals are considered to be real-valued vectors in an *N*-dimensional normed Euclidean vector space $\mathbb{R}^N$. For the purposes of CS, mainly the ℓ_0 and ℓ_1 norm are of importance. The sparsity k of a vector x is defined as the number of non-zero components, i.e., $\|x\|_0 = k$ .A vector x with sparsity k is said to be k-sparse .

Compressed sensing takes advantage of the sparsity of a signal $s \in \mathbb{R}^N$ in some fixed basis $\Psi \in \mathbb{R}^{N \times M}$ in order to recover it from a reduced measurement $y \in \mathbb{R}^M$, where $M < N$.

Acquiring a signal by CS consists of two main steps:

1) Measurement: apply a measurement matrix Φ to obtain the measurement y ,

$$y = \Phi s = \Phi\Psi x = Ax \tag{1}$$

with $s \in \mathbb{R}^N$ the original signal, $x \in \mathbb{R}^N$ its sparse decomposition, $\Psi \in \mathbb{R}^{N \times N}$ the fixed basis, $\Phi \in \mathbb{R}^{M \times N}$ the measurement matrix, $A = \Phi\Psi \in \mathbb{R}^{M \times N}$ the sensing matrix, and $y \in \mathbb{R}^M$ the measurement.

2) Recovery: exactly recover $\hat{s}$ from using y constrained ℓ_p -norm optimization,

$$\hat{x} = \arg\min_z \|z\|_p \qquad \text{s.t. } Az = y \tag{2}$$

$$\hat{s} = \Psi\hat{x} \tag{3}$$

with $p \in \{0,1\}$ in typical CS applications.

The actual choice of the ℓ_p norm in the recovery step (2), has considerable implications on the resulting solution $\hat{x}$ as well as on its computation. Firstly, using an ℓ_0 or ℓ_1 norm in the minimization problem will obviously lead to a sparser solution $\hat{x}$ compared to using ℓ_p norms with $p > 1$ .This is expected to provide a more accurate approximation for the sparse signal under consideration. Secondly, optimization problem (2) has distinct properties depending on the ℓ_p norm used in the minimization, and consequently requires distinct optimization methods. Considering ℓ_0 -norm minimization, the resulting optimization problem is non-convex, implying that one has to rely on greedy methods such as orthogonal matching pursuit (OMP) [13]. On the other hand, ℓ_1 -norm minimization also induces sparsity in the solution (albeit to a lesser extent than ℓ_0 -norm minimization) and has the advantage of leading to a convex optimization problem, which can be solved by convex optimization methods such as Basis Pursuit (BP) [14]. It is also possible to consider ℓ_p norms with $p \in \{0,1\}$, again leading to non-convex optimization problems.

2.2. Hyperspectral Image Compressed Sensing

There is a high inter-band correlation in hyperspectral image sequences (Figure 2 (a) and (b)), and current band image can be predicted by its adjacent band images. The entropy value of the residual image after de-correlation is small, as shown in Figure 2 (c). Compared with the current band image, the measurement data of de-correlation image is sparser, and more conducive to reconstruction. The detailed analysis is as follows.

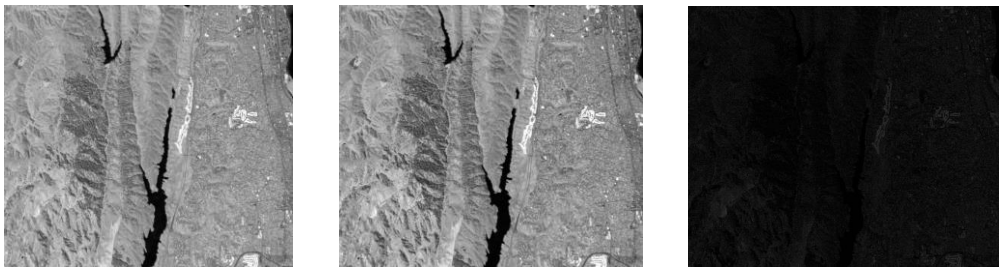

(a) 92th frame image (b) 93th frame image (c) residual image

Figure 2. Jasper Ridge Images and Residual Image

Set the current band image as x, the predicted band image as x_{LP}. x_{LP} is calculated by the inter-band linear prediction model, which will be described in the next section, and then the residual image can be expressed as $x_r = x - x_{LP}$; taking sparse transformation and random projection of x_r, then its measurement vector is:

$$y_r = \mathbf{\Phi\Psi}(x - x_{LP}) = y - \mathbf{\Phi\Psi}x_{LP} \tag{4}$$

where $\mathbf{\Phi}$ and $\mathbf{\Psi}$ are defined as Eq. (1); y represents the measurement vector of x. In the process of reconstruction, the current band image x is unknown, so we cannot obtain residual image x_r directly from x. But y is known, which was transformed from the encoder, and the reference image x_{ref}, which has been reconstructed and stored in frame memory is also known, so x_{LP} can be calculated by the inter-band linear prediction model. Then it is easy to obtain the measurement vector y_r by Eq. (4). The residual image x_r can be reconstructed by GPSR algorithm, which is usually used for solving a quadratic programming reformulation of a class of convex non-smooth unconstrained optimization problems arising in compressed sensing and other inverse problems in signal processing and statistics. The recovered residual image is set as $\hat{x}_r$, and then the finally recovered image $\hat{x}$ of current band image x is:

$$x = x_{LP} + x_r \tag{5}$$

The quality of current band recovered image $\hat{x}$ can be evaluated by Eq. (6):

$$\begin{aligned} \left\| x - \hat{x} \right\|_2 &= \left\| x - (x_{LP} + \hat{x}_r) \right\|_2 \\ &= \left\| x - (x_{LP} + x_r + e_r) \right\|_2 \\ &= \left\| (x - x_{LP}) - x_r - e_r \right\|_2 = \left\| e_r \right\|_2 \end{aligned} \tag{6}$$

where e_r is the reconstruction noise of residual image x_r. The equation above shows that the quality of current band recovered image is directly related to the reconstruction noise of residual image. The key idea of this approach is reconstructing the residual image instead of reconstructing the current band image directly, which will lead to higher reconstruction efficiency because the entropy value of the residual image is smaller and its measurement is sparser compared with that of the original one.

2.3. Block Linear Prediction Model

Prediction based on both the reference image and the predicted image with tight correlation can reduce redundancies effectively because the reference image provides a lot of information. Effective prediction model can improve the image quality of the reconstruction. Based on high inter-band correlation in hyperspectral images, a block liner prediction model is designed with regard to the real-time calculation, and detailed analysis is as follows.

It can be seen all the band images of hyperspectral image sequence have the same spatial structure; however, there are different correlations in different regions between adjacent bands, as shown in Figure 3. Therefore, the image is divided into some blocks B_i according to the gray values of different image regions and a simple line prediction model is constructed, as shown in Figure 4. For the block B_i, there is a linear relationship $f_n = af_{n-1} + d_i$ between the adjacent band f_{n-1} and f_n. In order to make the model simplified, we can set $a = 1$, thus:

$$f_n(x, y) = f_{n-1}(x, y) + d_i, \quad (x, y) \in B_i \tag{7}$$

Where $f_n(x, y)$ is the pixel gray value of row x and column y. In the block B_i:

$$\hat{d}_i = \frac{1}{N_i}\sum_{B_i} f_n(x,y) - \frac{1}{N_i}\sum_{B_i} f_{n-1}(x,y) \quad (x,y) \in B_i \tag{8}$$

N_i is the number of pixels in B_i ; the calculation of Eq. (8) is taken at the encoder side.

According to the d_i calculated by Eq. (8), the predicted image $f_{nLP}(x,y)$ of the current band can be obtained:

$$f_{nLP}(x,y) = f_{n-1}(x,y) + d_i \quad (x,y) \in B_i \tag{9}$$

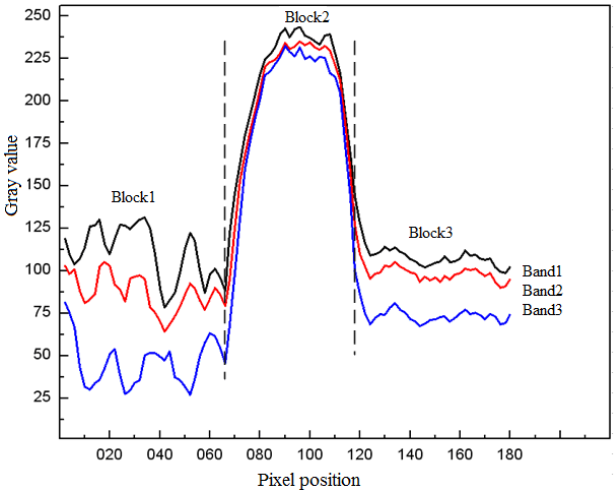

Figure 3. Correlation Between Adjacent Bands

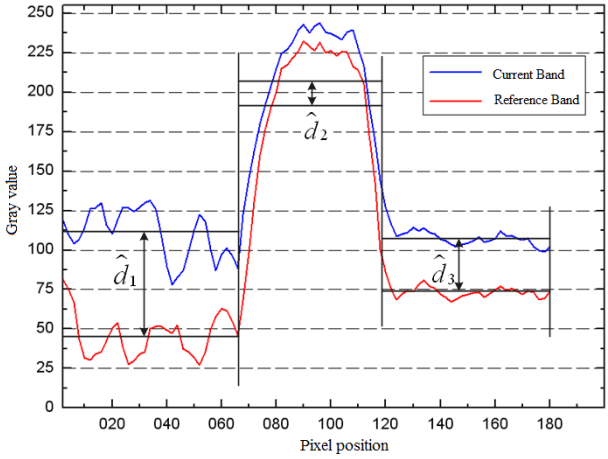

Figure 4. Inter-band Linear Prediction

2.4. Block Linear Prediction GPSR

The correlation between the adjacent bands of hyperspectral images is tight, but with the increase of distance, the correlation is weaker and weaker. Hence, we set five adjacent images as a group. Each group includes one reference image and four non-reference images, where the first one is reference image and the others are non-reference images.

The realizing process of block linear prediction GPSR (BLPG) is as follows.

Step1. At the encoder side, the reference image is observation projected and the linear prediction coefficients are calculated between the reference image and non-reference images.

Step2. At the decoder side, if the image is the first one in the group, it will be reconstructed directly by GPSR algorithm and then go to Step5, and else go to Step3.

Step3. Calculate the predicted image x_{LP} with block linear prediction model. Obtain the residual measurement vector y_r according to Eq. (4).

Step4. Recover the residual image x_r from y_r using GPSR algorithm, and calculate the non-reference recovered image x according to Eq. (5).

Step5. Store the recovered image in the frame memory.

Step6. Repeat Step 1 to Step 5, till all the images are processed.

3. Simulations

The experimental data of this paper are obtained from AIRIS hyperspectral remote sensing images, Jasper Ridge and Cuprite, provided by JPL laboratory. AVIRIS hyperspectral images are composed of 224 bands, of which the spectral range is from the visible to the near infrared (400-2500 nm), and each pixel is stored with 16 bit signed integer. The size of hyperspectral image from each group is 512(row) × 614(column) × 224 (band). For simplicity, only 512 × 512 rectangular area is selected to be the object of the experiment. Besides, due to the weaker correlation of adjacent frames in the Jasper Ridge sequence after the 150th frame, which cannot satisfy the prerequisite requirement of the proposed algorithm, only the first 150 frames of Jasper Ridge have been chosen as the experimental data.

In order to examine the performance of the proposed algorithm, four numerical experiments are carried out in the same platform (Intel 8-core 2GHZ/4G memory). (1) GPSR algorithm, sparse representation using 9/7 biorthogonal wavelets and decomposition stage is 4; (2) IAGP[15]; (3) distributed compressive video sensing (DCVS) algorithm proposed in literature[16]; (4) the proposed algorithm in this paper. The measurement rate is defined as MR=*M*/*N*, where *M* is the length of measurement vector, and *N* is the length of original signal.

Table 1 shows the average PSNR (Peak Signal to Noise Ratio) and the average runtime of the two experimental image sequences from MR=0.1 to MR=0.5 using different algorithms. In order to compare the experimental results easily, the data in Table 1 are displayed in Figure 4. From Figure 4(a) and (b), it is obvious that the BLPG algorithm can reconstruct image better. When MR=0.1, the average PSNR is 51.21dB for GPSR and 52.88dB for BLPG in Jasper Bridge sequence, where the average PSNR is increased by 1.67dB. When MR=0.5, the average PSNR is 56.32dB for GPSR and 60.31dB for BLPG in Jasper Bridge sequence, where the average PSNR is increased by 3.99dB. With the increase of MR, the average PSNR rises more obviously. The reason for this phenomenon is that the GPSR algorithm is a gradient projection (GP) algorithm applied to a quadratic program essentially, in which the search path from each iterate is obtained by projecting the negative-gradient direction onto the feasible set. The initial value of GPSR algorithm is a zero vector by default. When GPSR is used to reconstruct hyperspectral images, for each frame of the hyperspectral images, the GPSR iterative algorithm should start from zero vector and terminate iteration till the stopping criteria are satisfied. However, for the BLPG algorithm, most of the image information is obtained through image prediction, and only the residual image is recovered by GPSR. It is true that the residual image projection vector is sparser and closer to the zero vectors, and therefore recovering residual image with GPSR can get higher PSNR easily. DCVS has a better reconstruction quality compared with GPSR, but the average PSNR is

lower than BLPG, which is because in DCVS algorithm the inter-band correlation are applied only in the iterative initial frame and the iterative stopping criteria, which can improve the reconstruction performance to some extent. IAGP is an iteratively approximated gradient projection algorithm for sparse signal reconstruction, with a better reconstruction performance than GPSR, but as it ignores the correlation in hyperspectral images, the average PSNR is lower than DCVS.

Furthermore, as can be seen from Figure 5, the average runtime using DCVS is the shortest. The average runtime using BLPG algorithm is longer than that using DCVS, but shorter than that using GPSR and IAGP. This is because the BLPG algorithm makes full use of the characteristics of hyperspectral image, which has a tight correlation between the adjacent images and the pixel values of adjacent images are very close, thus the entropy value of the residual image is very small and the projection vector is sparser, which can accelerate the convergence speed and reduce the reconstruction time.

Table 1. Performance Comparison

Image Name	MR	Average PSNR (dB)				Average runtime (s)			
		GPSR	IAGP	DCVS	BLPG	GPSR	IAGP	DCVS	BLPG
Jasper Bridge	0.1	51.21	51.60	52.10	52.88	24.09	20.44	11.98	19.23
	0.2	52.51	53.56	54.51	55.31	22.12	17.93	10.77	16.49
	0.3	54.12	55.39	56.49	57.22	21.03	16.55	10.02	15.16
	0.4	55.36	56.71	57.86	58.89	19.78	15.16	9.86	14.41
	0.5	56.32	58.36	59.44	60.31	18.16	14.31	9.35	13.09
Cuprite	0.1	56.11	57.09	57.52	58.36	25.02	22.13	13.26	20.53
	0.2	58.78	59.33	60.56	61.42	23.78	20.06	12.61	19.39
	0.3	60.41	61.42	62.96	63.89	22.65	19.23	11.43	17.47
	0.4	62.95	64.36	65.73	67.43	21.96	17.88	10.92	15.25
	0.5	65.21	67.12	68.13	70.12	20.82	15.43	10.15	14.31

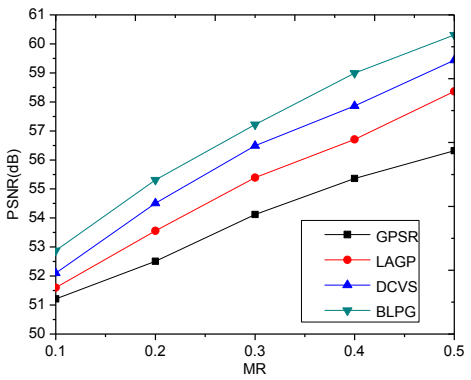

(a) Jasper Ridge average PSNR

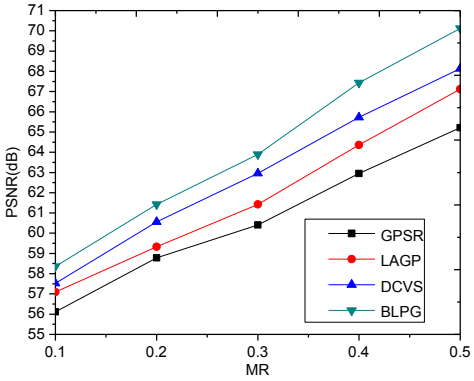

(b) Cuprite average PSNR

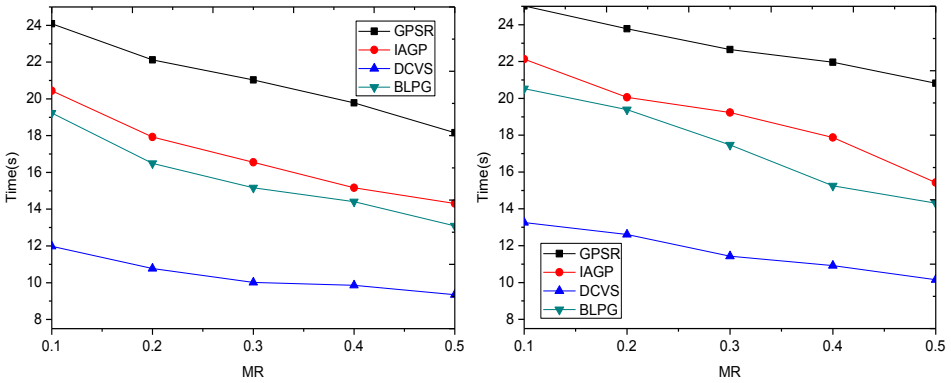

(c) Jasper Ridge Average Runtime (d) Cuprite Average Runtime

Figure 5. Performance Comparison

4. Conclusion

In this paper a novel hyperspectral image compression and reconstruction algorithm has been proposed based on compressed sensing. Our approach has two main innovations: 1) the theory of CS has been applied in image compression and reconstruction, which can greatly reduce the computational complexity and data storage at the encoder side; 2) the block linear prediction model has been used, which can reduce the redundancy between inter-band images. The entropy value of de-correlated image becomes smaller and its measurement is sparser. Therefore the quality of hyperspectral image reconstruction can be improved effectively. By the simulations it is indicated that the proposed approach can not only raise PSNR of the recovered image, but also reduce runtime. In a word, this approach has great value in application and is very suitable for the field of aerospace remote sensing.

References

[1] M. S. Kim, Y. R. Chen and P. M. Mehl, "Hyperspectral reflectance and fluorescence imaging system for food quality and safety", Transactions-American Society of Agricultural Engineers, vol. 44, no. 3, **(2001),** pp. 721-730.

[2] A. K. Rao and S. Bhargava,"Multispectral data compression using bidirectional inter band prediction", IEEE Trans. on Geoscience and Remote Sensing, vol. 34, no. 2, **(1996),** pp. 385-397.

[3] G. Liu and F. Zhao, "Efficient compression algorithm for hyperspectral images based on correlation coefficients adaptive 3D zerotree coding image processing", IET., vol. 2, no. 2, **(2008),** pp. 72-82.

[4] L. Yunsong, M. Jing and W. Chengke, "Three-Dimensional Orientation Prediction-Based Wavelet Transform for Interference Multi-Spectral Images Compression", Acta Optica Sinica，vol. 28, no. 12, **(2008)**.

[5] E. Candès, J. Romberg and T. Tao, "Robust uncertainty principles: Exact signal reconstruction from highly incomplete frequency information", IEEE Trans on Information Theory, vol. 52, no. 2, **(2006),** pp. 489-509.

[6] D. Donoho, "Compressed sensing", IEEE Trans. on Information Theory, vol. 52, no. 4, **(2006),** pp. 1289-1306.

[7] C. Rick and W. Yin, "Iteratively reweighted algorithms for compressive sensing", Acoustics, Speech and Signal Processing (ICASSP), **(2008)** March 31-April 4, pp. 3869-3872.

[8] G. Mohammad and P. Vandergheynst, "Hyperspectral image compressed sensing via low-rank and joint-sparse matrix recovery", Acoustics, Speech and Signal Processing (ICASSP), **(2012)** March 25-30, pp. 2741-2744, Kyoto, Japan.

[9] L. Haiying, L. Yunsong, Z. Jing, S. Juan and L. Pei, "Compressed hyperspectral image sensing with joint sparsity reconstruction", Satellite Data Compression, Communications, and Processing VII, **(2011)** September, pp. 815703-815703.

[10] X. Zhang, A. Wang, B. Zeng and L. Liu, Adaptive distributed compressed video sensing, Journal of Information Hiding and Multimedia Signal Processing, vol. 5, no. 1, **(2014)**, pp. 98-106.

[11] H. Chengfu, R. Zhang and D. Yin, "Compression technique for compressed sensing hyperspectral images", International Journal of Remote Sensing, vol. 33, no. 5, **(2012),** pp. 1586-1604.
[12] F. Mário, R. D. Nowak and S. J. Wright, "Gradient projection for sparse reconstruction: Application to compressed sensing and other inverse problems", IEEE Journal on Selected Topics in Signal Processing, vol. 1, no. 4, **(2007),** pp. 586-597.
[13] P. Y. Chandra, R. Rezaiifar, and P. S. Krishnaprasad, "Orthogonal matching pursuit: Recursive function approximation with applications to wavelet decomposition", Signals, Systems and Computers, **(1993),** pp. 40-44.
[14] S. S. Chen, D. L. Donoho and M. A. Saunders, "Atomic decomposition by basis pursuit", SIAM J. Sci. Comput., vol. 20, no. 1, **(1998),** pp. 33-61.
[15] Z. Liu, Z. Wei and W. Sun, "An iteratively approximated gradient projection algorithm for sparse signal reconstruction". Applied Mathematics and Computation, vol. 228, **(2014),** pp. 454-462**.**
[16] L. W. Kang, C. S. Lu, "Distributed compressive video sensing", Acoustics, Speech and Signal Processing, **(2009),** pp. 1169-1172.

Authors

Xu Cheng received B.Sc. and M.Sc degrees both from Nanjing University of Aeronautics & Astronautics in 2005 and 2010, respectively. Currently he is a Ph.D. candidate in Nanjing University of Aeronautics & Astronautics. His research interests are image compression and computer vision in the field of aerospace.

Huang Daqing is currently a professor and doctoral supervisor in Nanjing University of Aeronautics & Astronautics. His main research interests are optical measurement and telemetry.

Han Wei received B.Sc. in communication engineering from Liao Cheng University. Currently he is a Ph.D. candidate in Nanjing University of Aeronautics & Astronautics. Her research interests are image compression and signal processing.

